

The deconfining phase transition in D=2+1 SU(N) gauge theories

Jack Little^a and Michael Teper^b

^aFakultat für Physik, Universität Bielefeld, D-33615 Bielefeld, Germany

^bRudolf Peierls Centre for Theoretical Physics, University of Oxford,
1 Keble Road, Oxford OX1 3NP, UK

Abstract

We study the deconfining transition of SU(N) gauge theories in 2+1 dimensions for $2 \leq N \leq 8$. We confirm that the transition is second order for $N \leq 3$ and first order for $N \geq 5$. For the more delicate case of SU(4) all our evidence points to the transition being weakly first order. After extrapolating to the continuum limit, we obtain a deconfining temperature that can be well fitted by $T_c/\sqrt{\sigma} = 0.9026(23) + 0.880(43)/N^2$ for all $N \geq 2$.

1 Introduction

In 2+1 dimensions, $SU(N)$ gauge theories have a coupling g^2 that has dimensions of mass. Thus the dimensionless coupling appropriate to physics on a length scale l is $g^2 l$: that is to say, the theory becomes free in the ultraviolet, and strongly coupled in the infrared. Moreover the theory is found to be linearly confining (see [1] and references therein) although no analytic proof exists. These properties are reminiscent of $D = 3 + 1$ gauge theories, and so $D = 2 + 1$ gauge theories have received much attention in the hope that they might provide a useful stepping stone between the soluble $D = 1 + 1$ case, and the physically interesting $D = 3 + 1$ case.

In this paper we calculate some properties of the deconfining transition in $D = 2 + 1$ $SU(N)$ gauge theories. We use standard lattice methods, extrapolate to the continuum limit, and then perform a large N extrapolation that enables us to extend our results to all values of N . These calculations parallel similar calculations in $D = 3 + 1$ [2].

There exist older calculations for $SU(2)$ and $SU(3)$ (see for example [3]) as well as more recent work on $SU(4)$ [4, 5, 6] and $SU(5)$ [7, 5] most of which appeared while this work was in progress. Most of our calculations have appeared in [8] which contains various details omitted in this paper, and a summary of our early results was presented in [5]. The main change in this paper is that we use a more accurate calculation of the string tension [1] to provide the scale in which to express the quantities we calculate, and we examine the delicate case of $SU(4)$ in greater detail.

2 Lattice setup

Our calculations are performed using standard lattice techniques. We work on periodic cubic $L_s^2 \times L_t$ lattices with lattice spacing a . The degrees of freedom are $SU(N)$ matrices, U_l , assigned to the links l of the lattice. The partition function is

$$Z(\beta) = \int \prod_l dU_l e^{-\beta \sum_p \{1 - \frac{1}{N} \text{ReTr} U_p\}} \quad (1)$$

where U_p is the ordered product of matrices around the boundary of the elementary square (plaquette) labelled by p . In the continuum limit

$$\beta = \frac{2N}{ag^2} \quad (2)$$

where g^2 is the coupling, which in $D = 2 + 1$ has dimensions of mass. This is the standard Wilson plaquette action and the continuum limit is approached by tuning $a \rightarrow 0$ and hence $\beta = 2N/ag^2 \rightarrow \infty$. One expects that for large N physical masses will be proportional to the 't Hooft coupling $\lambda \equiv g^2 N$ [9], and this is indeed what one observes [10]. So if we vary $\beta \propto N^2$ then we are keeping the lattice spacing a fixed in physical units, to leading order in N .

When $L_s \rightarrow \infty$ at fixed L_t and fixed β , the field theory is at a temperature

$$T = \frac{1}{a(\beta)L_t}. \quad (3)$$

As is conventional, we use eqn(3) to define T at finite $L_s \gg L_t$ as well. By increasing β at fixed L_t we increase T so as to locate the critical value $\beta = \beta_c$ at which the system deconfines: $T_c(a) = 1/a(\beta_c)L_t$. (We shall often write this as T_c if there is no ambiguity.) An ‘order’ parameter we shall use is the plaquette, u_p , averaged over the space time volume,

$$\bar{u}_p = \frac{1}{N_p} \sum_p u_p \quad ; \quad u_p = \frac{1}{N} \text{ReTr} U_p \quad (4)$$

where $N_p = 3L_s^2L_t$ is the total number of plaquettes. Another parameter is the Polyakov loop

$$l_p(x) = \text{Tr} \prod_{t=1}^{L_t} U_t(x, t) \quad ; \quad \bar{l}_p = \frac{1}{L_s^2} \sum_x l_p(x). \quad (5)$$

3 Methodology

In this Section we briefly describe how we calculate the properties of the deconfining phase transition. For a more detailed review, with references, see for example [11].

Consider the specific heat on a $L_s^2L_t$ lattice, defined conventionally by

$$\frac{1}{\beta^2} C(\beta) \equiv \frac{\partial}{\partial \beta} \langle \bar{u}_p \rangle = N_p \langle \bar{u}_p^2 \rangle - N_p \langle \bar{u}_p \rangle^2. \quad (6)$$

Suppose that there is a first order deconfining transition at β_c so that $\langle \bar{u}_p \rangle$ jumps from $\langle \bar{u}_{p,c} \rangle$ to $\langle \bar{u}_{p,d} \rangle$ as we increase β through β_c . On our finite spatial volume, V , the jump becomes a crossover. Let us choose the maximum of $C(\beta)$ as defining the critical β at finite volume: $\beta_c(V)$. Up to the weakly varying factor of β^{-2} this coincides with the point at which $\langle \bar{u}_p \rangle$ changes fastest with β . It is easy to see that for large enough V this is the value of β at which the system is equally likely to be in the confined and deconfined phases and that

$$\lim_{V \rightarrow \infty} \frac{1}{\beta_c^2} C(\beta_c(V)) = \frac{N_p}{4} (\langle \bar{u}_{p,c} \rangle - \langle \bar{u}_{p,d} \rangle)^2 \propto VL_h^2. \quad (7)$$

Thus at a first order transition the specific heat diverges linearly in V and the limiting value of $C(\beta)/V$ is directly related to the latent heat L_h . Now, the crossover exists over a region of T where there is a finite probability for the system to be in both the confined and deconfined phases. Assuming that the free energies of the two phases are smooth as one passes through T_c , this implies that the crossover extends over a range of $O(1/V)$ in T and hence that any definition of T_c within this range will generically have a leading $O(1/V)$ correction at large V . So we expect that as $V \rightarrow \infty$

$$\frac{T_c(\infty) - T_c(V)}{T_c(\infty)} = \frac{\beta_c(\infty) - \beta_c(V)}{\beta_c(\infty)} = \frac{h}{VT_c^2} = h \left(\frac{L_t}{L_s} \right)^2 \quad (8)$$

(where we have used $T = 1/aL_t = \beta g^2/2NL_t$). Moreover, because the free energy $\propto N^2$, we also expect that

$$h \stackrel{N \rightarrow \infty}{\propto} \frac{1}{N^2} \quad (9)$$

Thus if we calculate $\beta_c(V)$ from the maximum of $C(\beta)$, and do so for several V , we can use eqn(8) to extrapolate to $V = \infty$, thus obtaining $\beta_c(V = \infty)$. We can then use the results of [1] to obtain the string tension at this β , and hence $T_c(a)/\sqrt{\sigma(a)}$ at $a = 1/L_t T_c$. We now repeat the exercise for several other values of L_t and perform an extrapolation of this ratio to the continuum limit. In the same way we can use eqn(7) to obtain the continuum value of the latent heat, e.g. L_h/T_c^3 .

If the transition is second order, there is no discontinuity in $\langle \bar{u}_p \rangle$ but there is a diverging correlation length. Rewriting eqn(6) as an integrated correlation function

$$\frac{1}{\beta^2} C(\beta) = \sum_p \langle (\bar{u}_p - \langle \bar{u}_p \rangle) (\bar{u}_{p_0} - \langle \bar{u}_p \rangle) \rangle \quad (10)$$

(where p_0 is an arbitrary plaquette) we see that at the transition $C(\beta)$ will diverge as $V \rightarrow \infty$, with a power that depends on how the correlation length diverges with increasing V , i.e. on the critical exponents. The maximum of $C(\beta)$ is where the correlation length is largest (up to weak corrections) and provides a natural definition of $\beta_c(V)$. Using a conventional notation, the leading large volume behaviour is

$$\frac{1}{\beta^2} C(\beta) = c_0 V^{\frac{\alpha}{\nu d}} + c_1 \quad (11)$$

and

$$\frac{T_c(\infty) - T_c(V)}{T_c(\infty)} = \frac{\beta_c(\infty) - \beta_c(V)}{\beta_c(\infty)} = \frac{h}{(V T_c^2)^{\frac{1}{\nu d}}} = h \left(\frac{L_t}{L_s} \right)^{\frac{2}{\nu d}} \quad (12)$$

We can use this to obtain $\beta_c(\infty)$ from our finite V calculations, then use [1] to transform this into a value of $T_c(a)/\sqrt{\sigma(a)}$, then repeat all this for several values of L_t , and finally extrapolate to the continuum limit.

In practice using the plaquette and the specific heat is not the most accurate method. For our second order transitions the excitation whose mass vanishes typically has a weak overlap with the plaquette, so that it contributes a small peak to $C(\beta)$ unless the volume because extremely large. For our first order transitions the discontinuity is on physical length scales, so $(\langle \bar{u}_{p,c} \rangle - \langle \bar{u}_{p,d} \rangle) \sim O(a^3)$ and once again one has to go to very large V to see a strong effect in $C(\beta)$.

For these reasons it is usual to also use the susceptibility of the Polyakov loop

$$\frac{\chi}{V} = \langle |\bar{l}_p|^2 \rangle - \langle |\bar{l}_p| \rangle^2. \quad (13)$$

In the confined phase the Polyakov loop fluctuates about zero while in the deconfined phase it fluctuates about a non-zero value proportional to an element of the center of $SU(N)$. One uses $|\bar{l}_p|$ rather than \bar{l}_p since even in the deconfined phase the latter will (strictly speaking) average to zero for finite V through tunnelling between the N (Euclidean) vacua. While taking the modulus might seem like an ad hoc fix, in fact it is closely related to the adjoint Polyakov loop: $\text{Tr}_A l_p \propto |\text{Tr}_F l_p|^2 - 1$. The latter is a more natural and general ‘order’ parameter than

the usual fundamental Polyakov loop. For example, it will serve equally well if we decide to express the gauge fields in the adjoint representation. For large N it vanishes as $1/N^2$ in the confined phase, and is unsuppressed in the deconfined phase. For these reasons it would make sense to use a susceptibility based on the adjoint Polyakov loop. However, given that the definition in eqn(13) is now customary, we shall adhere to it in this paper. Just as for $C(\beta)$, we can define a $\beta_c(V)$ from the maximum of χ/V and extrapolate it to $V = \infty$ using eqn(8) or eqn(12) depending on the order of the transition. The value of χ/V at its maximum is not directly related to a physical quantity, unlike $C(\beta)$, so we do not consider its infinite volume extrapolation.

The reason that χ/V provides a better signal for the phase transition than $C(\beta)$ is that the ground state of the flux loop that winds around the temporal torus becomes massless as $T \rightarrow T_c^-$ if the transition is second order. (This mass is an eigenstate of a transfer matrix along a spatial direction.) The Polyakov loop is an operator with a projection on this state. The fact that near T_c excited flux loops are relatively massive, and that the projection on the ground state is quite good, for the range of a we work with, means that the effect of the vanishing mass on χ/V is very pronounced. For a first order transition, on the other hand, the discontinuity in the average Polyakov loop is not directly related to a physical energy density and so is not as small as for the plaquette. As $\beta \rightarrow \infty$ Polyakov loops do get renormalised to zero, and using χ/V becomes more difficult, but for our range $a \in [1/2T_c, 1/5T_c]$ these problems are not severe and accurate calculations are easy to perform.

We therefore base our calculations of β_c on χ/V . However we do use $C(\beta)$ to obtain the latent heat in those cases where the extrapolation in eqn(7) can be usefully performed. To do so we recall that the energy density is given by

$$\frac{\bar{E}}{V} = -\frac{1}{V} \frac{\partial}{\partial \frac{1}{T}} \ln Z = \frac{T^2}{V} \frac{\partial}{\partial T} \ln Z, \quad (14)$$

where we use $Z = \sum_s \exp\{-E_s/T\}$, while

$$N_p \langle u_p \rangle = \frac{\partial}{\partial \beta} \ln Z = \frac{\partial T}{\partial \beta} \frac{\partial}{\partial T} \ln Z + \frac{\partial V}{\partial \beta} \frac{\partial}{\partial V} \ln Z \quad (15)$$

where the first equality in eqn(15) uses the expression in eqn(1) for Z . Noting that the volume derivative gives the pressure, and that the pressure of the two phases is equal at $T = T_c$, we see that the contribution of this second term to

$$\Delta_{u_p} \equiv \langle u_{p,c} \rangle - \langle u_{p,d} \rangle \equiv \langle \bar{u}_{p,c} \rangle - \langle \bar{u}_{p,d} \rangle \quad (16)$$

will vanish at $T = T_c$. Thus the latent heat, L_h , which is the difference of the energy densities in the two phases at $T = T_c$, can be written, using eqns(14,15,16) and $T = 1/aL_t$, as

$$\frac{L_h}{T_c^3} = -3L_t^3 a \frac{\partial \beta}{\partial a} \Delta_{u_p} \simeq 3L_t^3 \beta \Delta_{u_p} \quad (17)$$

where at the last step we use the asymptotic expression $\beta = 2N/ag^2$. As we see from eqn(7), the quantity Δ_{u_p} , and hence the latent heat, is given by the $V \rightarrow \infty$ limit of the specific heat.

The expression in eqn(17) is not unique. We can do better by noting that $a\partial\beta/\partial a = (a\mu)\partial\beta/\partial(a\mu)$ where we choose for μ some physical quantity whose lattice value has been accurately calculated over a wide range of β (e.g. the string tension). Now parameterise the variation of $a\mu$ with β as a series in $1/\beta$, evaluate $(a\mu)\partial\beta/\partial(a\mu)$ and substitute in eqn(17). This will improve over using $\beta = 2N/ag^2$ by at least an additional $O(1/\beta)$ correction. Having said that, we shall use the cruder estimate in eqn(17) because our relatively large errors on L_h do not demand a more sophisticated treatment.

For some L_t our range of V is not large enough to calculate L_h from the specific heat. In those case we take a sequence of lattice fields generated close to $T = T_c$, and identify long subsequences that are in either the confined or deconfined phase, using the value of \bar{l}_p to do so. We then obtain $\langle u_{p,c} \rangle$ and $\langle u_{p,d} \rangle$ from the appropriate subsequences, and hence Δ_{u_p} . This direct method of calculating Δ_{u_p} has the advantage of weak finite volume corrections and so does not require an explicit extrapolation to $V = \infty$. However there are systematic errors to do with the assignment of lattice fields to a particular phase, and these errors only become small on large volumes where tunnelling between phases become relatively rare. Finally, using eqn(17) we transform our value of Δ_{u_p} into a value for the latent heat.

An aside. Although one might imagine that the calculations in $D = 2 + 1$ would be easier than in $D = 3 + 1$ this is not really so. For example, one requirement that a first order transition should be well defined in a practical calculation is that the rate of tunnelling should be small enough for the co-existence of the ordered and disordered phases to be readily visible. This rate is governed by a factor $\exp\{-2\sigma_{cd}L_s^{D-2}/T_c\} = \exp\{-2\sigma^0(L_s/L_t)^{D-2}\}$ where σ_{cd} is the interface tension and we have written $\sigma_{cd} = \sigma^0 T_c^{D-1}$. This factor gives the suppression of those intermediate configurations in a tunnelling where the volume is split into two co-existing phases by domain walls that extend right across the lattice. So all other things being equal, i.e. if the dimensionless tension σ^0 is the same, then the size L_s/L_t in 2 space dimensions should equal the square of the size, $(L_s/L_t)^2$, in 3 space dimensions in order to achieve the same tunnelling suppression. So the typical factor $L_s/L_t \sim 3$ in $D = 3 + 1$ needs to become a much more challenging $L_s/L_t \sim 10$ in $D = 2 + 1$. For reasons like this, the accuracy and range of our calculations is not much more impressive than in $D = 3 + 1$ [2].

4 Results

The basic step is to calculate the maximum of χ/V , or $C(\beta)$, for some given values of N , L_t and L_s . To do so we typically evaluate χ/V at 4 or more values of β . These values are judiciously chosen so as to straddle the maximum and to be close enough to that maximum for each Monte Carlo run to have a usefully large number of tunnelling events between confined and deconfined phases. (All this clearly requires some preparatory work.) To obtain the maximum accurately we need a smooth interpolation between the calculated values, and this is provided by standard reweighting techniques (see [12] and Appendix A of [8]). In Fig. 1 we show an example of such a reweighted curve, for a $25^2 3$ lattice in $SU(6)$.

We now present our results. We begin with $SU(2)$ and $SU(3)$ where the deconfinement transitiona are well known to be second order [3]. We then deal with $SU(N \geq 5)$ where they

turn out to be clearly first order. Finally we dwell in more detail on the delicate case of SU(4). In each case we perform calculations for $L_t = 2, 3, 4, 5$ and from these we obtain the continuum limit of $T_c/\sqrt{\sigma}$ and (where relevant) L_h/T_c^3 . The continuum limit can be obtained from a standard weak coupling extrapolation of the form

$$\frac{aT_c(a)}{a\sqrt{\sigma(a)}} = \frac{T_c(a)}{\sqrt{\sigma(a)}} = \frac{T_c(0)}{\sqrt{\sigma(0)}} + c_1 a^2 \mu^2 + c_2 a^4 \mu^4 + \dots \quad (18)$$

Here μ is some convenient physical energy scale, such as $\sqrt{\sigma}$ or T_c , in which case $a^2 T_c^2 = 1/L_t^2$. The string tension is obtained by interpolation of the results presented in [1]. In the final subsection we examine the N -dependence of these quantities as well as the scaling of finite volume corrections.

One might reasonably worry that at $L_t = 2$ the lattice spacing is too coarse for the weak coupling expansion in eqn(18) to be applicable. (In units of T_c it will be $a = 0.5T_c$.) In fact there is a strong-to-weak coupling crossover in $D = 2 + 1$ SU(N) gauge theories that becomes a phase transition at $N = \infty$ [13] in a manner very similar to the Gross-Witten transition in $D = 1 + 1$ [14]. This transition occurs at a value of β that is about 10% below $\beta_c(L_t = 2)$. Thus it is not excluded that at this β a weak-coupling expansion is applicable. We also note that for light glueball masses the ratio $m_G/\sqrt{\sigma}$ appears to be described by such a weak-coupling expansion at comparable values of β [10, 15]. For these reasons we shall (cautiously) attempt continuum extrapolations from $L_t = 2$.

4.1 SU(2) and SU(3)

It is known from earlier calculations [3] that both SU(2) and SU(3) have second order deconfining transitions, and there is good evidence that these are in the universality classes of the $2D$ $q = 2$ and $q = 3$ state Potts models respectively, as one would expect from the general arguments of [16]. Our calculations corroborate the second order nature of the transitions. As an example we show in Fig. 2 a histogram of values of \bar{l}_p as obtained in SU(2) on a $90^2 \times 3$ lattice at $\beta = 4.9$, which is very close to $\beta_c(L_t = 3)$. We observe a single broad distribution which shows no sign of the two peak structure that would indicate co-existing phases.

For each value of $L_t = 1/aT_c$ in the range $L_t \in [2, 5]$ we calculate $\beta_c(V)$ for several values of V and extrapolate to $V = \infty$ using eqn(12) with $\nu = 1, 5/6$ for $N = 2$ and $N = 3$ respectively. (These being the exponents of the relevant Potts models [17].) We show an example of such an extrapolation in Fig. 3; it is for SU(2) and $L_t = 3$. In Table 1 we list the values of $\beta_c(V = \infty)$ for SU(2) that have been obtained in this way, and the range of volumes used in each extrapolation. We also give the value of the string tension [1] that corresponds to each $\beta_c(V = \infty)$ for each L_t . (The error on $a\sqrt{\sigma}$ includes the error on β_c .) From this we obtain the values of $T_c/\sqrt{\sigma} = 1/a\sqrt{\sigma}L_t$ shown in Table 1. In Table 2 we display the corresponding results for SU(3).

4.2 SU($N \geq 5$)

For $N = 5$ it is known that the transition is first order [7, 5] and our calculations show that this is the case up to $N = 8$. We find that the strength of the transition is ‘normal’ and that the latent heat is approximately constant for $N \geq 5$. This provides convincing evidence for the claim that the transition remains first order for larger N and, in particular, for $N = \infty$.

To illustrate the first order nature of the transition we show in Fig. 4 a histogram of values of \bar{l}_p as obtained in SU(8) on a 20^23 lattice at value of β which is very close to $\beta_c(L_t = 3)$. We observe a pronounced two peak structure that clearly indicates the co-existence of ordered and disordered phases. Moreover one finds that this two-peak structure becomes more pronounced with increasing V .

For each value of $L_t = 1/aT_c$ in the range $L_t \in [2, 5]$ we calculate $\beta_c(V)$ for several values of V and extrapolate to $V = \infty$ using eqn(8). We show an example of such an extrapolation in Fig. 5; it is for SU(6) and $L_t = 3$. In Tables 4, 5, 6 we list the values of $\beta_c(V = \infty)$ that have been obtained in this way, and the ranges of volumes used in each extrapolation. We also give the values of the string tension [1] that correspond to each $\beta_c(V = \infty)$ for each L_t . From this we obtain the values of $T_c/\sqrt{\sigma} = 1/a\sqrt{\sigma}L_t$ shown in the Tables.

In Table 7 we list our fitted value of the coefficient h of the $O(1/V)$ correction to $\beta_c(V)$ in eqn(8).

To obtain the specific heat, L_h , as given by eqn(17), we calculate the quantity Δ_{u_p} defined in eqn(16). For small L_t we can obtain it from the specific heat peak as in eqn(7). For larger L_t this becomes inaccurate and we obtain it by identifying sequences of confined and deconfined lattice fields, as described at the end of Section 3. Our results are listed in Table 8. Values obtained from the specific heat are labelled by a star. In most cases where we have values from both methods, they are reasonably consistent. In one case this is clearly not so: this serves as a warning that, at least for this rather delicate quantity, our claimed control of systematic errors is likely to be optimistic.

4.3 SU(4)

If the SU(4) transition were second order, one would expect [16, 4] it to be in the universality class of the symmetric Ashkin-Teller model (see [18] for a recent review) of which the $q = 4$ Potts model is a special case. This has continuously varying critical exponents and logarithmic effects which, as emphasised in [4], creates difficulties in the analysis. The results of [4], favoured the Potts model class, although their $L_t = 2$ transition appeared to be first order. Our preliminary results [5] pointed to the transition remaining first order at larger L_t and this was confirmed by our more extensive calculations in [8]. A simultaneous recent study of this question presents quite convincing evidence that the transition is first order [7]. In this paper we present some of our results from [8] as well as some from larger volumes.

We begin by showing the histogram of the Polyakov loop on very large volumes, at our smallest values of the lattice spacing. In Fig. 6 we show the results obtained on a 60^25 lattice and in Fig. 7 those obtained on a 120^25 lattice. We see a clear 2-peak structure reflecting the co-existence of ordered and disordered phases. The structure becomes more pronounced

as L_s/L_t increases from 12 to 24 and V increases by a factor of 4. The gap between the two maxima does not appear to shrink significantly as V increases. All this provides rather strong evidence that the transition is first order and remains so in the continuum limit.

In Fig. 8 we show an extrapolation of $\beta_c(V)$ assuming an $O(1/V)$ correction that assumes it is indeed first order. As we see, such first order finite size scaling works very well. In Table 3 we list our extrapolated values of $\beta_c(V = \infty)$, and the corresponding values of $T_c/\sqrt{\sigma}$. In Table 7 we list the coefficient of the $O(1/V)$ correction in eqn(8). Finally in Table 8 we list the values of the discontinuity in the average plaquette across the transition. These will translate into values of the specific heat through eqn(17).

4.4 continuum limits

To extrapolate our calculated values of $T_c/\sqrt{\sigma}$ to the continuum limit we use eqn(18) with $a\mu = a\sqrt{\sigma}$. We could equally well choose to use $a\mu = aT_c = 1/L_t$, and we have checked that the results of the two types of fits are within one standard deviation of each other. (We also find that the quality of the fits is comparable.) In Table 9 we show the results of two such fits: one is an $O(a^4)$ extrapolation to $L_t \geq 2$ and the second is an $O(a^2)$ extrapolation to $L_t \geq 3$. One finds that $O(a^2)$ extrapolations to $L_t \geq 2$ are statistically unacceptable.

The best fits are rather poor, but not unacceptable, for SU(2) and SU(3) and this presumably reflects the presence of a very smooth strong-weak coupling crossover at these smaller values of N . For SU(5) the fit is extremely poor, and this is due entirely to our $L_t = 5$ value. As we see in Table 7 the fitted coefficient of the $O(1/V)$ correction is anomalously large. It seems clear that this value happens to be out by several standard deviations. We therefore also show a fit (denoted by a \star) that uses the values of $\beta_c(V = \infty)$ given in [7] for $L_t = 3, 4, 5$ together with our value for $L_t = 2$ (since this is not calculated in [7]). This gives a fit with an acceptable χ^2 . In fact our values for $L_t = 3, 4$ are consistent with those of [7]; it is only our $L_t = 5$ value that is anomalous. This is reflected in the fact that the continuum extrapolation of our results is very similar to that obtained using the values of [7], as we see in Table 9. What we can therefore say is that for larger N one has good $O(a^4)$ continuum extrapolations even from $L_t = 2$. As an example, we display the SU(8) case in Fig. 9. The residual systematic error reflected in the small difference between the $O(a^2)$ and $O(a^4)$ fits would be removed by calculations at slightly larger L_t .

Turning now to the latent heat, we find that we can obtain good continuum extrapolations from $L_t \geq 2$ using just a $O(a^2)$ correction:

$$\frac{1}{T_c(a)} \left(\frac{L_h(a)}{N^2} \right)^{\frac{1}{3}} = \frac{1}{T_c(0)} \left(\frac{L_h(0)}{N^2} \right)^{\frac{1}{3}} + c_1 a^2 \sigma. \quad (19)$$

We normalise by T_c because that is a characteristic energy scale of the transition, and by N^2 because one expects $L_h \propto N^2$ at large N . We choose to take the third root so that we extrapolate a dimensionless ratio that is of the form $[m]/[m]$. The results are shown in Table 10.

The values of the coefficient h at larger values of L_t are too inaccurate, as we see from Table 7 to allow an attempt at a useful continuum extrapolation of that quantity.

4.5 N dependence

In Fig. 10 we plot the continuum latent heat, in units of T_c and normalised to N^2 , against $1/N^2$, which is expected to be the leading correction to the $N = \infty$ limit. We obtain a good fit to $N \geq 5$ with

$$\frac{1}{T_c} \left(\frac{L_h}{N^2} \right)^{\frac{1}{3}} = 0.459(7) - \frac{0.21(24)}{N^2}. \quad (20)$$

It is not possible to include the SU(4) value. Indeed in our natural units, the SU(4) latent heat L_h is about one-half of its value at larger N , where the variation with N is essentially negligible. That is to say, the deconfining transition in SU(4) is weakly first order.

The result of attempting to fit our continuum values of $T_c/\sqrt{\sigma}$ with just a leading $O(1/N^2)$ correction is shown in Fig. 11. (We use the values obtained by $O(a^4)$ extrapolations from $L_t \geq 2$.) It is remarkable that one obtains a good fit

$$\frac{T_c}{\sqrt{\sigma}} = 0.9026(23) + \frac{0.880(43)}{N^2} \quad (21)$$

to all values of $N \geq 2$ despite the fact that the $N = 2, 3$ transitions are second order and the remainder are first order.

It is interesting to see if the finite volume effects disappear with N^2 , as one expects if the free energies and interface tensions scale as $\propto N^2$. A relevant quantity is the parameter h that is the coefficient of the $O(1/V)$ correction to the V -dependence of T_c . As we see from Table 7 the errors are too large at larger L_t to allow a continuum extrapolation. Instead we take the values at $L_t = 3$, i.e. $aT = 1/3T_c$, where the errors are still small and a is perhaps not too coarse. Plotting the corresponding values of hN^2 in Fig. 12 we see very nice evidence that finite volume corrections vanish as $h \propto 1/N^2$ just as counting arguments suggest.

5 Conclusions

We have found that, just as in $D = 3 + 1$ [2], SU(N) gauge theories in $D = 2 + 1$ have a deconfining transition that is second order at low N and first order at larger N . Again as in $D = 3 + 1$ [2], one finds that the variation with N of $T_c/\sqrt{\sigma}$ is small and that, quite remarkably, one can fit this ratio for all $N \geq 2$ with just a leading $O(1/N^2)$ correction with a modest coefficient, as we see in Fig. 11.

We have seen that the SU(4) transition is almost certainly first order, although weakly so, as we see from its suppressed latent heat in Fig. 10. This is reminiscent of $D = 3 + 1$ where it is the SU(3) transition that is weakly first order.

When expressed in a natural normalisation, the value of the latent heat at larger N is $L_h \sim N^2 \times (0.46T_c)^3$. By contrast, in $D = 3 + 1$ it is considerably larger [2]: $L_h \sim N^2 \times (0.8T_c)^4$. This is perhaps natural given that the thermal gluons at high T have more degrees of freedom in three space dimensions than in two. But one should also note that if we express L_h in units of $\sqrt{\sigma}$ rather than T_c , most of this difference goes away.

The fact that the value of $T_c/\sqrt{\sigma}$ is ~ 1.5 times larger in $D = 2+1$ than in $D = 3+1$ is quite natural, and already occurs for the simple Nambu-Goto string model where the deconfining (Hagedorn) transition occurs at $T_c^2 = 3/\pi(D - 2)$ [1, 19]. This simply reflects the differing entropy of strings or flux tubes in 2 and 3 spatial dimensions.

It is obviously interesting to ask if the gluon plasma immediately above the phase transition is strongly coupled, as it has been found to be in $D = 3 + 1$ both experimentally and theoretically. (See [20] and references therein.) Here the effective dimensionless 't Hooft coupling on the scale T_c will be

$$\frac{g^2 N}{T_c} \sim \frac{g^2 N}{\sqrt{\sigma}} \sim 5 \quad (22)$$

using the values in [1]. This is large enough to raise the possibility of a ‘strongly coupled gluon plasma’ in $D = 2 + 1$ and to motivate a numerical exploration, but that goes beyond the scope of the present paper.

Acknowledgements

We have had useful discussions with B. Bringoltz and F. Bursa during the course of this work. We are grateful to Ph. de Forcrand for critical discussions on the SU(4) transition and for encouraging us to strengthen our numerical results for that case. The computations were performed on resources funded by Oxford and EPSRC. Jack Liddle’s contribution was performed at Oxford and was supported by PPARC.

References

- [1] B. Bringoltz, M. Teper Phys. Lett. B645 (2007) 383 [hep-th/0611286].
- [2] B. Lucini, M. Teper and U. Wenger, Phys. Lett. B545 (2002) 197 [hep-lat/0206029]; JHEP 0401 (2004) 061 [hep-lat/0307017]; JHEP 0502 (2005) 033 [hep-lat/0502003].
- [3] J. Engels et al, Nucl. Phys. Proc. Suppl. 53 (1997) 420 [hep-lat/9608099].
M. Teper, Phys. Lett. B313 (1993) 417.
J. Christensen, G. Thorleifsson, P. Damgaard and J. Wheeler, Nucl.Phys.B374:225-248,1992.
J. Christensen and P. Damgaard, Nucl. Phys. B348 (1991) 226-256.
- [4] Ph. de Forcrand and O. Jahn, hep-lat/0309153.
- [5] J. Liddle and M. Teper, PoS LAT2005 (2005) 188 hep-lat/0509082
- [6] K. Holland, M. Pepe and U-J Wiese, arXiv:0712.1216.
- [7] K. Holland, JHEP 0601 (2006) 023 [hep-lat/0509041]
- [8] J. Liddle, D. Phil Thesis, Oxford 2006.

- [9] G. 't Hooft, Nucl. Phys. B72 (1974) 461.
E. Witten, Nucl. Phys. B160 (1979) 57.
S. Coleman, 1979 Erice Lectures.
- [10] M. Teper, Phys. Rev. D59 (1999) 014512 [hep-lat/9804008].
- [11] Hildegard Meyer-Ortmanns, Rev. Mod. Phys. 68 (1996) 473 [hep-lat/9608098].
- [12] A. Ferrenberg and R. Swendsen, Phys. Rev. Lett. 63 (1989) 1195.
- [13] F. Bursa and M. Teper, Phys. Rev. D74 (2006) 125010 [hep-th/0511081].
- [14] D. Gross and E. Witten, Phys. Rev. D21 (1980) 446.
- [15] B. Lucini and M. Teper, Phys. Rev. D66 (2002) 097502 [hep-lat/0206027].
B. Bringoltz and M. Teper, in preparation.
- [16] B. Svetitsky and L. Yaffe, Nucl. Phys. B210 (1982) 423.
- [17] F. Wu, Rev. Mod. Phys. 54 (1982) 235.
- [18] J. Salas and A. Sokal, J. Stat. Phys. 85 (1996) 297 [hep-lat/9511022].
- [19] B. Bringoltz and M. Teper, Phys.Rev. D73 (2006) 014517 [hep-lat/0508021].
- [20] B. Bringoltz and M. Teper, Phys. Lett. B628 (2005) 113 [hep-lat/0506034].

SU(2)				
aT_c	$L_s \in$	β_c	$a\sqrt{\sigma}$	$T_c/\sqrt{\sigma}$
$\frac{1}{2}$	[15,60]	3.4475(36)	0.4902(13)	1.0200(27)
$\frac{1}{3}$	[22,90]	4.943(13)	0.3164(10)	1.0535(33)
$\frac{1}{4}$	[30,80]	6.483(26)	0.2317(11)	1.0790(51)
$\frac{1}{5}$	[50,85]	8.143(57)	0.1799(14)	1.1117(87)

Table 1: Critical β at various values of $L_t = 1/aT_c$, with resulting values of $T_c/\sqrt{\sigma}$. String tensions from [1]. All for SU(2).

SU(3)				
aT_c	$L_s \in$	β_c	$a\sqrt{\sigma}$	$T_c/\sqrt{\sigma}$
$\frac{1}{2}$	[15,60]	8.1489(31)	0.5641(17)	0.8864(27)
$\frac{1}{3}$	[23,90]	11.3711(91)	0.35730(54)	0.9329(14)
$\frac{1}{4}$	[30,120]	14.717(17)	0.26098(41)	0.9579(15)
$\frac{1}{5}$	[40,70]	18.131(61)	0.20517(79)	0.9748(38)

Table 2: As in Table 1 but for SU(3).

SU(4)				
aT_c	$L_s \in$	β_c	$a\sqrt{\sigma}$	$T_c/\sqrt{\sigma}$
$\frac{1}{2}$	[13,30]	14.8403(26)	0.5840(38)	0.8562(56)
$\frac{1}{3}$	[20,45]	20.377(11)	0.37254(52)	0.8948(13)
$\frac{1}{4}$	[30,60]	26.228(75)	0.27195(95)	0.9193(32)
$\frac{1}{5}$	[37,60]	32.154(71)	0.21423(56)	0.9336(25)

Table 3: As in Table 1 but for SU(4).

SU(5)				
aT_c	$L_s \in$	β_c	$a\sqrt{\sigma}$	$T_c/\sqrt{\sigma}$
$\frac{1}{2}$	[12,20]	23.5315(58)	0.5973(19)	0.8371(27)
$\frac{1}{3}$	[18,25]	32.065(21)	0.37912(58)	0.8792(14)
$\frac{1}{3}$		32.0765(54)*	0.37888(52)	0.8798(12)
$\frac{1}{4}$	[24,36]	41.057(36)	0.27729(40)	0.9016(13)
$\frac{1}{4}$		41.113(12)*	0.27682(30)	0.9031(10)
$\frac{1}{5}$	[30,40]	50.67(16)	0.21626(80)	0.9248(34)
$\frac{1}{5}$		50.275(20)*	0.21823(22)	0.9165(10)

Table 4: As in Table 1 but for SU(5).

SU(6)				
aT_c	$L_s \in$	β_c	$a\sqrt{\sigma}$	$T_c/\sqrt{\sigma}$
$\frac{1}{2}$	[10,20]	34.1848(52)	0.6033(35)	0.8288(48)
$\frac{1}{3}$	[15,25]	46.395(17)	0.38058(94)	0.8759(22)
$\frac{1}{4}$	[20,30]	59.372(48)	0.27883(46)	0.8966(15)
$\frac{1}{5}$	[30,37]	72.59(24)	0.21975(88)	0.9101(36)

Table 5: As in Table 1 but for SU(6).

SU(8)				
aT_c	$L_s \in$	β_c	$a\sqrt{\sigma}$	$T_c/\sqrt{\sigma}$
$\frac{1}{2}$	[5,14]	61.245(11)	0.60688(92)	0.8239(13)
$\frac{1}{3}$	[10,20]	82.704(43)	0.38525(54)	0.8652(12)
$\frac{1}{4}$	[10,18]	105.52(11)	0.28190(43)	0.8868(14)
$\frac{1}{5}$	[12,25]	128.30(28)	0.22332(61)	0.8956(25)

Table 6: As in Table 1 but for SU(8).

h				
aT_c	SU(4)	SU(5)	SU(6)	SU(8)
$\frac{1}{2}$	0.275(14)	0.190(15)	0.132(7)	0.0567(20)
$\frac{1}{3}$	0.390(39)	0.239(36)	0.188(13)	0.079(11)
$\frac{1}{4}$	0.50(19)	0.212(50)	0.204(29)	0.066(16)
$\frac{1}{5}$	0.88(24)	0.71(15)	0.25(14)	0.052(29)

Table 7: The coefficient of the $O(1/V)$ term in the variation of $\beta_c(V)$ in eqn(8).

Δ_{u_p} at $T = T_c$				
L_t	SU(4)	SU(5)	SU(6)	SU(8)
2	0.00603(9) [*] 0.00631(37) [†]	0.00886(11) [*]	0.01118(10) [*]	0.01238(9) [*]
3	0.00073(8) ^{*†} 0.00087(6)	0.00117(12) [*] 0.00125(4) [†]	0.00138(9) ^{*†}	0.00206(6) [*] 0.00146(3) [†]
4	0.00024(5)	0.000336(9)	0.000352(20)	0.000377(24)
5	0.00010(1)	0.000140(5)	0.000148(4)	0.000157(8)

Table 8: The difference between the average plaquette in the confined and deconfined phases at $T = T_c$. Entries with a \star are calculated from the specific heat. Where there are two values, the \dagger indicates the value used in the continuum fit of the latent heat.

continuum limit								
N	$O(a^4)$ fit $L_t \geq 2$				$O(a^2)$ fit $L_t \geq 3$			
	$T_c/\sqrt{\sigma}$	c_1	c_2	χ^2/n_{df}	$T_c/\sqrt{\sigma}$	c_1	χ^2/n_{df}	
2	1.1238(88)	-0.87(14)	1.83(45)	3.3	1.1224(90)	-0.70(15)	3.3	
3	0.9994(40)	-0.65(6)	0.94(15)	2.1	0.9890(31)	-0.44(4)	1.9	
4	0.9572(39)	-0.56(5)	0.76(13)	0.1	0.9516(33)	-0.41(3)	0.5	
5	0.9404(38)	-0.53(5)	0.68(11)	8.2	0.9325(28)	-0.38(3)	11.1	
5 [*]	0.9380(19)	-0.49(3)	0.58(8)	0.9	0.9337(14)	-0.38(2)	3.4	
6	0.9300(48)	-0.46(7)	0.51(16)	1.1	0.9228(35)	-0.33(4)	1.0	
8	0.9144(41)	-0.38(5)	0.38(11)	0.4	0.9114(25)	-0.31(3)	0.1	

Table 9: Continuum limits of $T_c/\sqrt{\sigma}$ for various N , using either a $O(a^4)$ or $O(a^2)$ formula, with values of the coefficients of the lattice corrections, and the quality of fit.

latent heat		
N	$\frac{1}{T_c} \left(\frac{L_h}{N^2}\right)^{\frac{1}{3}}$	χ^2/n_{df}
4	0.393(13)	1.4
5	0.448(4)	1.4
6	0.459(4)	0.9
8	0.453(4)	0.9

Table 10: Continuum limit of the latent heat using an $O(a^2)$ extrapolation to $2 \leq L_t \leq 5$.

$T_c/\sqrt{\sigma}$ vs N								
		$O(1/N^4)$ fit				$O(1/N^2)$ fit		
	$N \geq$	$N = \infty$	c_1	c_2	χ^2/n_{df}	$N = \infty$	c_1	χ^2/n_{df}
a^4	2	0.9035(41)	0.85(11)	0.12(31)	0.23	0.9026(23)	0.88(5)	0.18
a^2	2	0.9016(26)	0.76(7)	0.46(33)	0.70	0.8989(17)	0.85(4)	0.98
a^2	3	0.8977(38)	0.94(14)	-1.0(1.1)	0.07	0.9007(20)	0.81(5)	0.35

Table 11: Results of fitting the N -dependence of $T_c/\sqrt{\sigma}$ either to $O(1/N^4)$ or to $O(1/N^2)$. Results shown separately for the different extrapolations to the continuum limit.

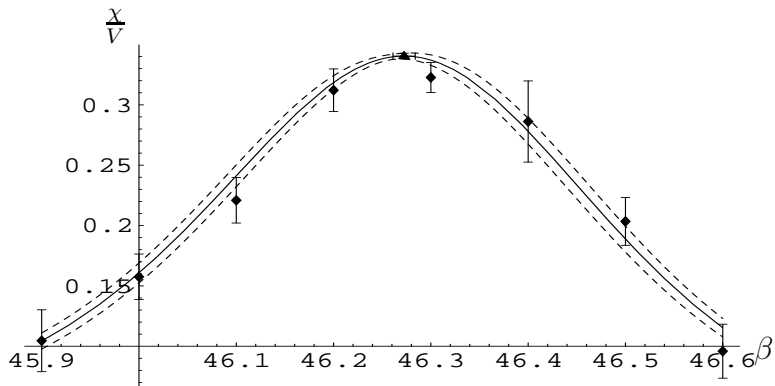


Figure 1: An example of reweighting: the Polyakov loop susceptibility χ/V versus β in SU(6) on a $25^2 3$ lattice.

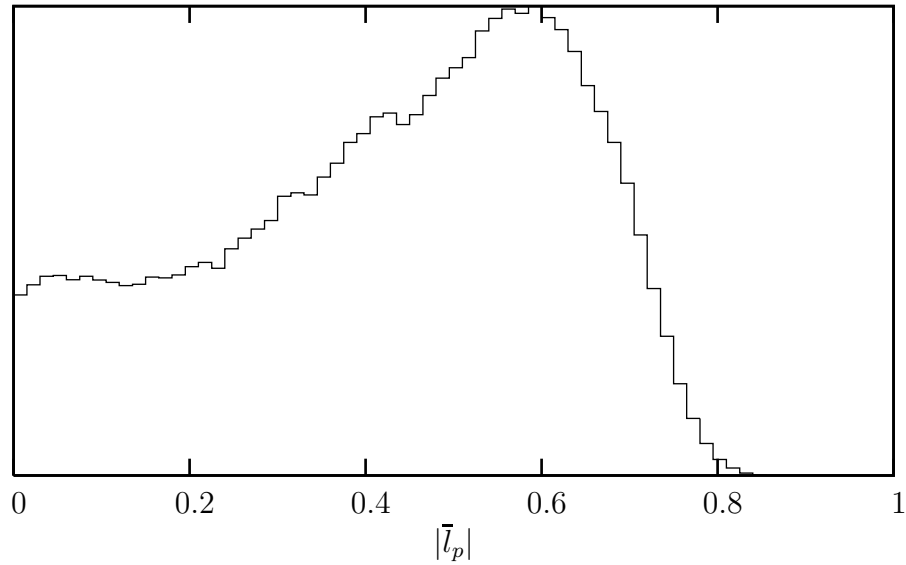


Figure 2: Number of lattice fields, N , with a given value of the Polyakov loop $|\bar{l}_p|$. In SU(2), at $\beta = 4.9$, on a $90^2 3$ lattice.

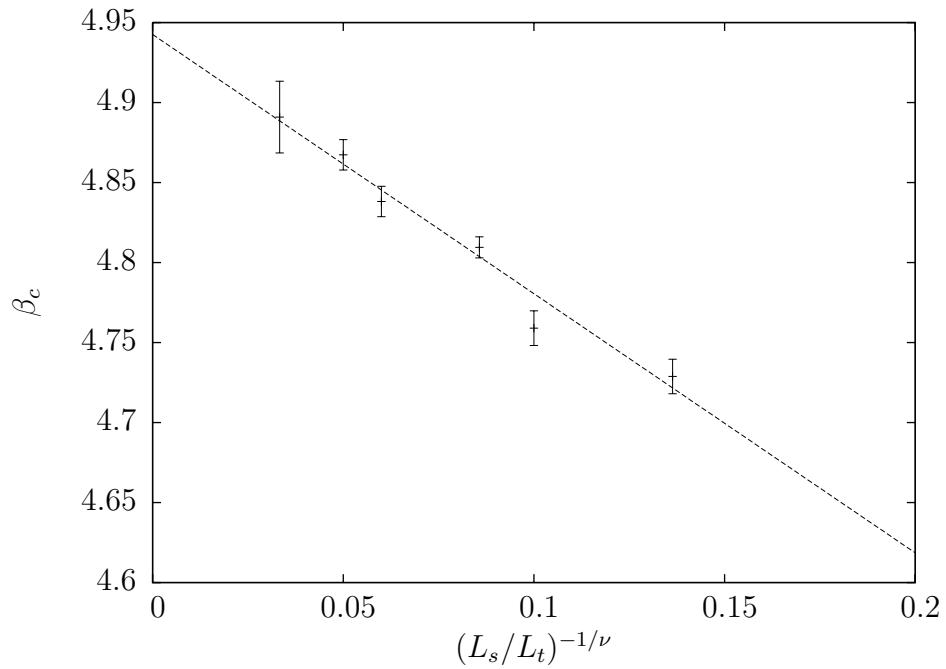


Figure 3: A plot of the critical coupling $\beta_c(V)$ against $(L_s/L_t)^{-1/\nu}$ with an extrapolation to $V = \infty$. In SU(2) for $aT_c = 1/L_t = 1/3$.

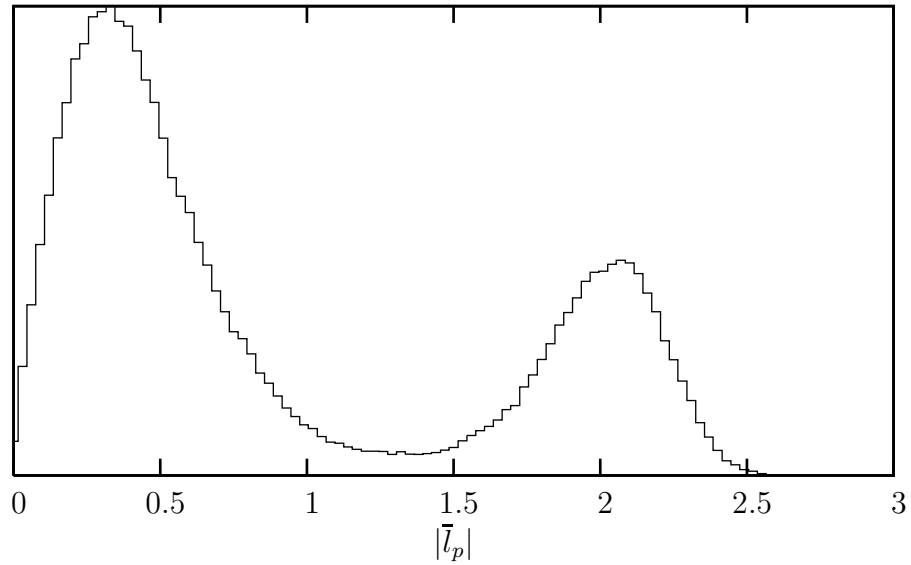


Figure 4: Number of lattice fields, N , with a given value of the Polyakov loop $|\bar{l}_p|$. In SU(8), at $\beta = 82.5$, on a 20^23 lattice.

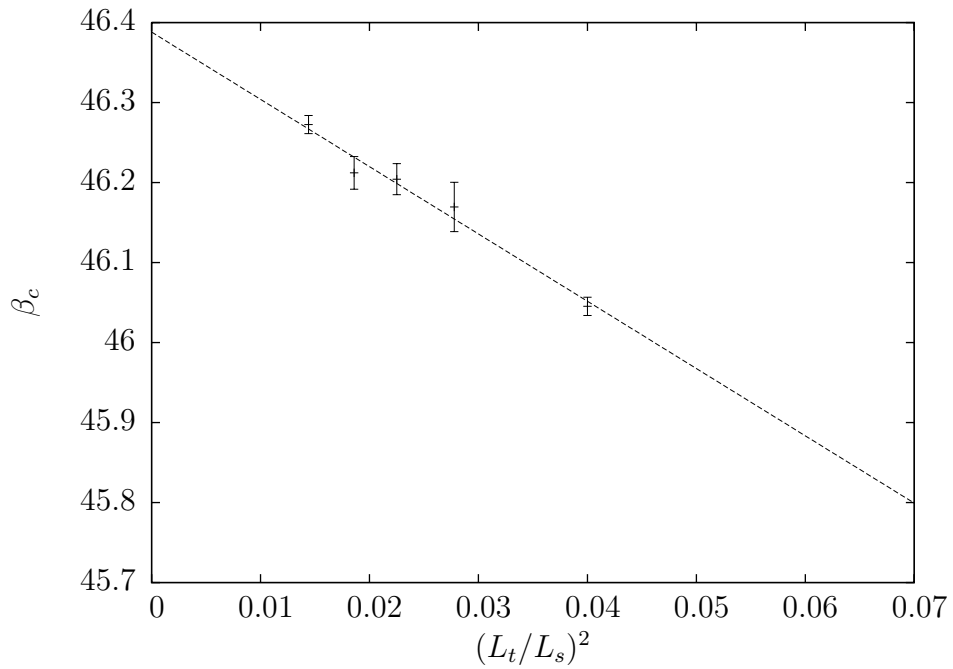


Figure 5: A plot of the critical coupling $y = \beta_c(V)$ against $x = (L_s/L_t)^2$ with an extrapolation to $V = \infty$. In SU(6) for $aT_c = 1/L_t = 1/3$.

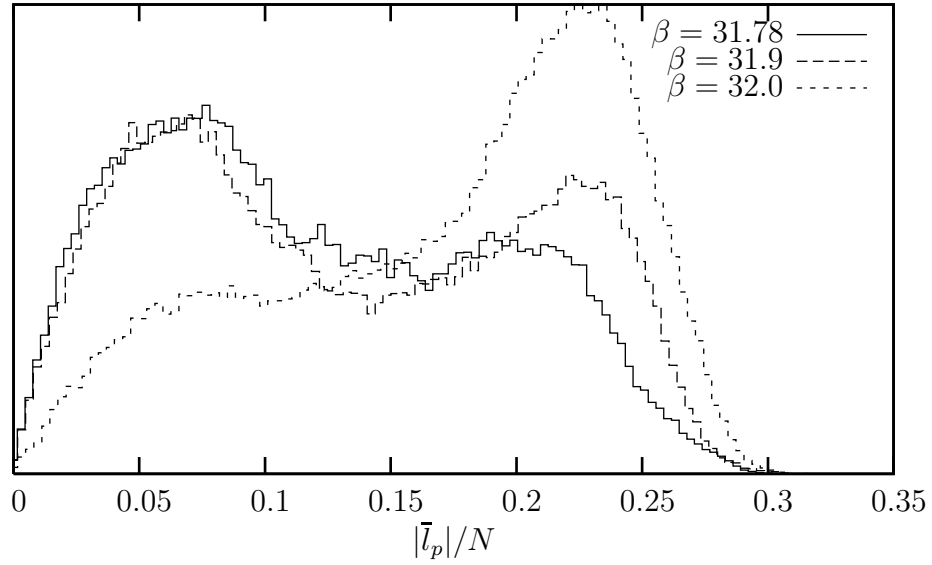


Figure 6: Histogram of the number of lattice fields with a given value of the Polyakov loop $|\bar{l}_p|/N$. In SU(4), at the β indicated, on a 60^{25} lattice.

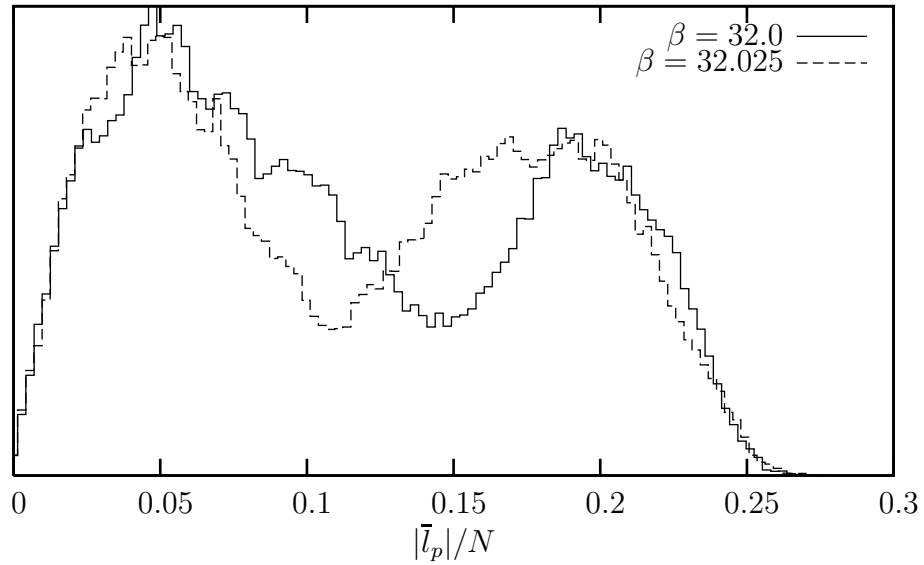


Figure 7: Histogram of the number of lattice fields with a given value of the Polyakov loop $|\bar{l}_p|/N$. In SU(4), at the β indicated, on a 120^{25} lattice.

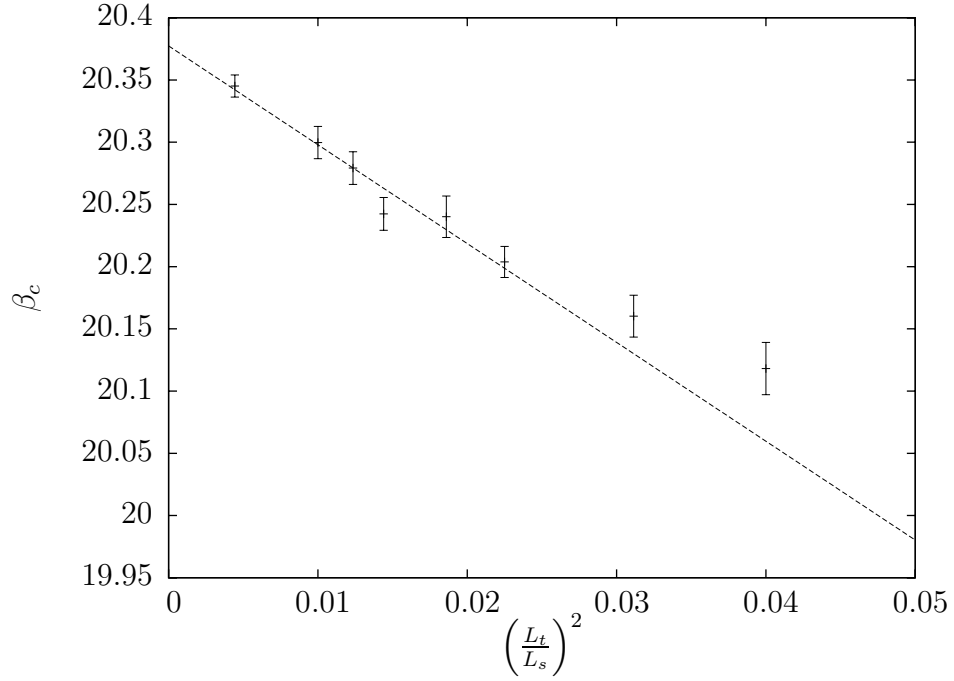


Figure 8: A plot of the critical coupling $y = \beta_c(V)$ against $x = (L_s/L_t)^2$ with an extrapolation to $V = \infty$. In SU(4) for $aT_c = 1/L_t = 1/3$.

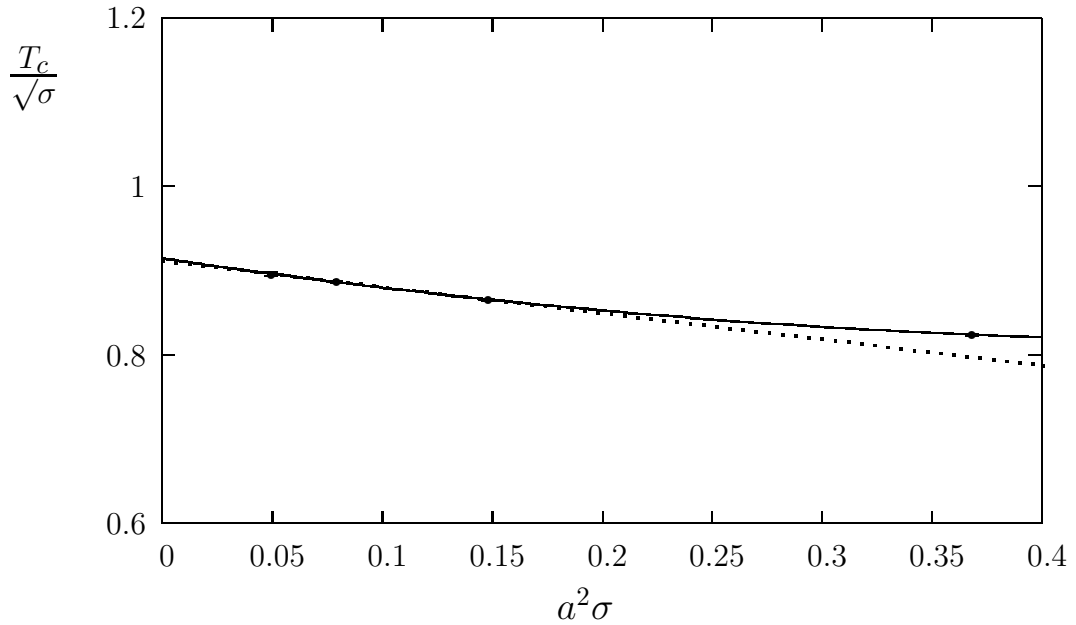


Figure 9: Values in SU(8) of $T_c(a)/\sqrt{\sigma(a)}$ plotted against $a^2\sigma$ and extrapolated to the continuum limit using either linear (...) or quadratic (-) extrapolations.

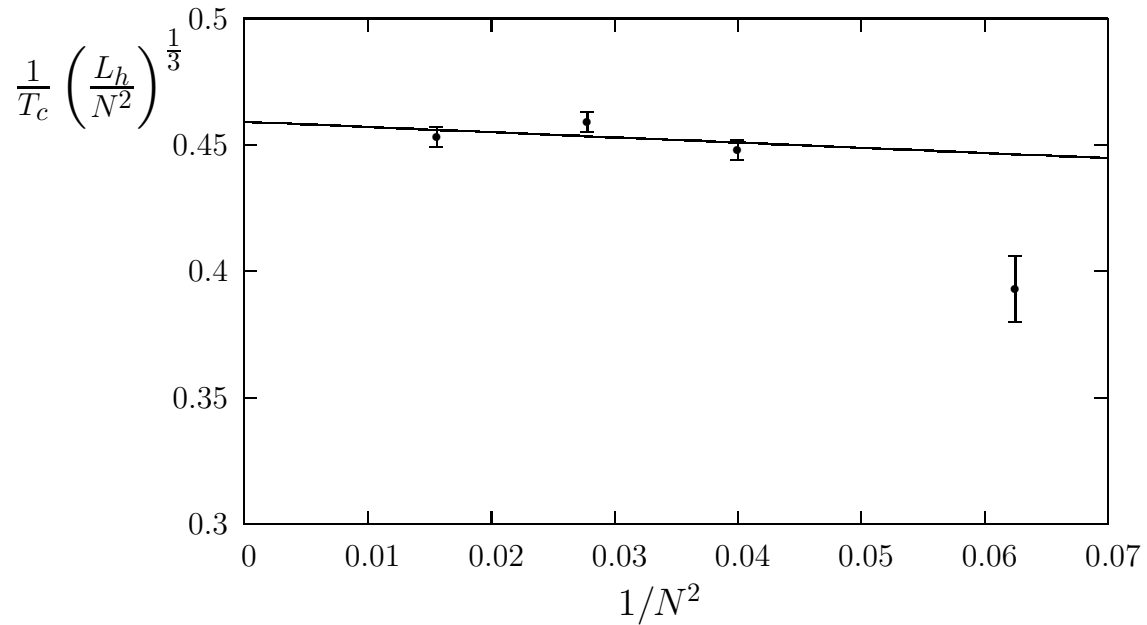


Figure 10: Latent heat, with a natural normalisation, obtained at a fixed lattice spacing $a = 1/3T_c$. The fit to large N uses a leading $O(1/N^2)$ correction.

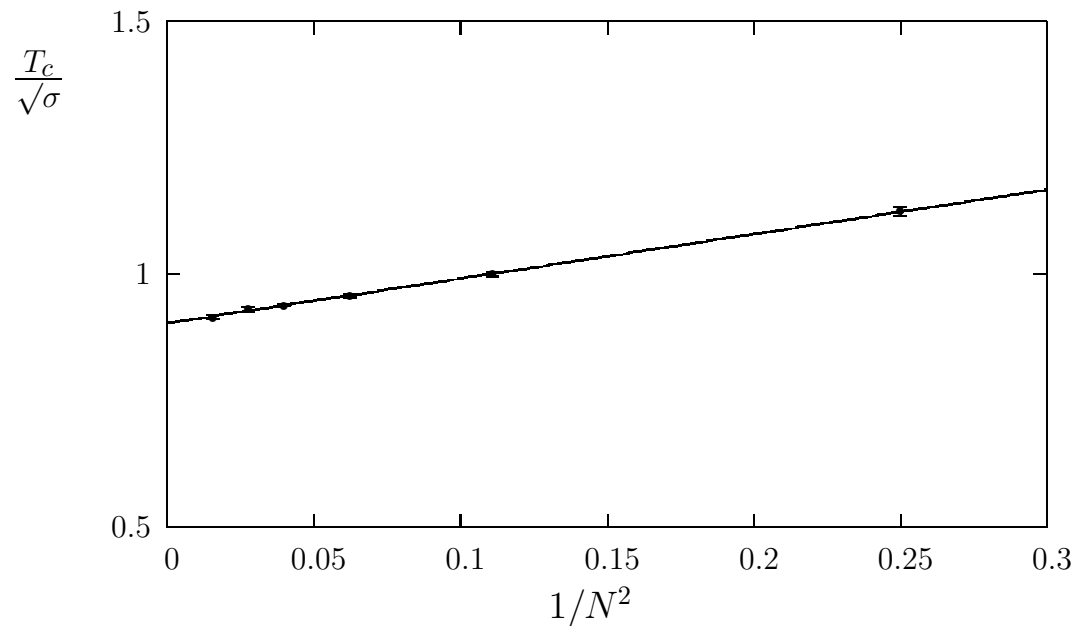


Figure 11: Continuum values of $T_c/\sqrt{\sigma}$ plotted against $1/N^2$. The fit to all N uses just a leading $O(1/N^2)$ correction.

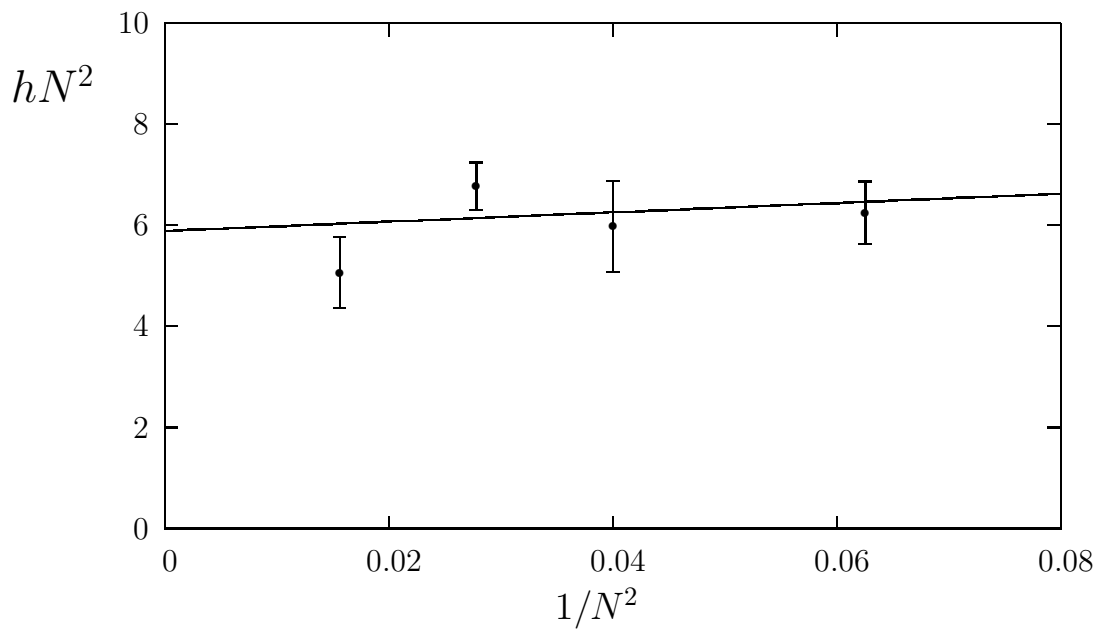


Figure 12: N -dependence of the coefficient h of the $O(1/V)$ correction to $\beta_c(V)$, obtained at a fixed lattice spacing $a = 1/3T_c$.